EVALUATION OF PERFORMANCE OF DIAPHRAGM WALLS BY WALL DEFLECTION PATHS

Richard N. Hwang [1], Tsung-Yeh Lee [2], Chung-Ren Chou [3], and Ting-Chiun Su [4]

ABSTRACT

The performance of diaphragm walls in excavation for Shandao Temple Station of Taipei Metro is evaluated by using the concept of wall deflection path which is a plot of maximum wall deflections versus depth of excavation. Finite element analyses were performed and parameter studies were carried out to illustrate the sensitivity of various factors on the results. Based on the results obtained, the baseline wall deflection path is established for excavations in the T2 Zone of the Taipei Basin. It can be used in future as the basis for evaluating the influence of factors which affect wall deflections.

Key words: Deep excavation, diaphragm wall deflection, finite element analyses.

1. INTRODUCTION

The concept of wall deflection path and reference envelope was first introduced in Moh and Hwang (2005) and subsequently discussed in Hwang *et al*. (2006). Applications of this concept in evaluating the performance of diaphragm walls in the Taipei Basin were later illustrated in Hwang and Moh (2007a; 2007b; 2008) and Hwang *et al*. (2007a; 2007c). Numerical analyses have been conducted by Hsiung and Hwang (2009a; 2009c) and Chao *et al*. (2010) to substantiate the concept and to study the sensitivity of various parameters on wall deflections.

This study is an extension of the above-mentioned studies aiming at generalization of the conclusions reached therein by supporting data obtained from additional numerical analyses. Furthermore, the baseline wall deflection path for the T2 Zone (Moh and Associates, 1987; Lee, 1996) is established and the performance of walls is evaluated accordingly.

2. WALL DEFLECTION PATH AND REFERENCE ENVELOPE

In congested cities, there are most likely structures adjacent to excavations and, hence, wall deflections are inevitably affected. This is particularly true for excavations for underground stations and cut-and-cover tunnels, which are normally constructed underneath major streets with many high-rise buildings alongside, of metro systems. These high-rise buildings normally have basements together with retaining structures left in-place after the completion of construction, hence, deflections of walls in nearby excavations are very likely to be reduced as a result. Furthermore, there are always entrances, ventilation shaft, *etc*., structurally connected to the station walls and, therefore, the rigidity of the walls is much increased and wall deflections are much reduced. Since the structures adjacent to excavations are normally omitted in back analyses, comparison of the results obtained in back analyses with the observed performance of such walls is unfair and often leads to mis-judgment. It is therefore desirable to have a means to quantify the influence of adjacent structures, and also many other factors which may affect wall deflections, so the performance of walls can be faithfully evaluated.

Figure 1 shows the "wall deflection paths", which are plots of observed maximum wall deflections versus depth of excavation at various stages of excavation in a log-log scale for walls of 1m in thickness in deep excavations in the T2 Zone (Moh and Hwang 2005). The numerals in the legends refer to the site numbers and the alphabets refer to individual inclinometers. For example, "9A" refers to inclinometer A at Site 9, *etc*. Also shown in the figure is the so-called "reference envelope" of these paths. As suggested in Moh and Hwang (2005), reference envelopes are established by taking into account the data points in the range of depths of 10 m and 20 m only and are defined by Δ_4 and Δ_{100} which are the maximum wall deflections for depths of excavation of 4 m and the wall deflections projected to a depth of excavation of 100 m, respectively. Accordingly, the reference envelope shown can be defined by $\Delta_4 = 10$ mm and $\Delta_{100} = 400$ mm.

As depicted in Fig. 2, wall deflection paths can generally be categorized into 5 types, *i.e.*, Types *A* to *E*, which will be discussed in detail in Section 4. If the baseline wall deflection path, which is the wall deflection path for excavations in green field without the influence of factors other than soil conditions, is available for a particular site, the influence of many factors can be identified and evaluated by comparing the wall deflection paths observed with this baseline deflection path. Therefore, it is desirable to establish baseline wall deflection paths for different geological zones as a basis for evaluating the performance of walls.

3. CASE STUDIED

To this aim, the performance of the diaphragm walls observed during excavation for constructing Shandao Temple Station (BL8 Station) of Bannan Line of the Taipei Metro is studied herein. Figure 3 shows the configuration of the station and the locations of instruments relevant to this study.

Manuscript received May 12, 2011; revised December 2, 2011; accepted January 15, 2012.

[1] Senior Specialist (corresponding author), Moh and Associates, Inc., New Taipei City, Taiwan (e-mail: richard.hwang@maaconsultants.com).

[2] Engineer, Moh and Associates, Inc., New Taipei City, Taiwan.

[3] Senior Engineer, Moh and Associates, Inc., New Taipei City, Taiwan.

[4] Senior Manager, Moh and Associates, Inc., New Taipei City, Taiwan.

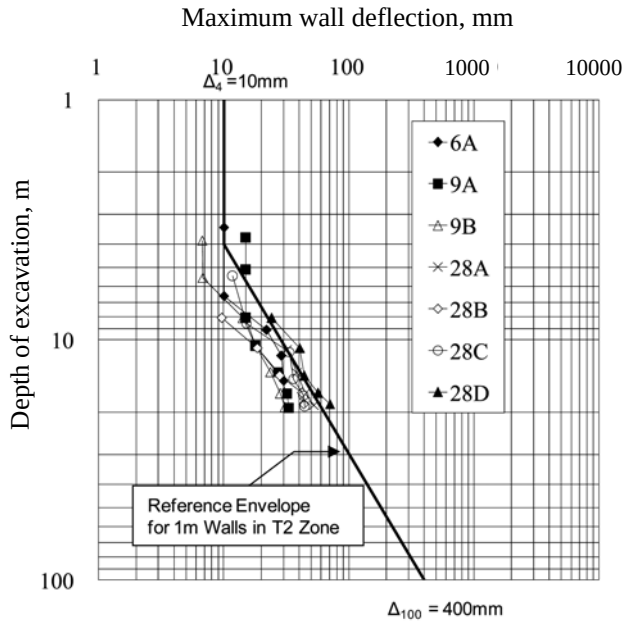

Fig. 1 Wall deflection paths and reference envelope in the T2 Zone

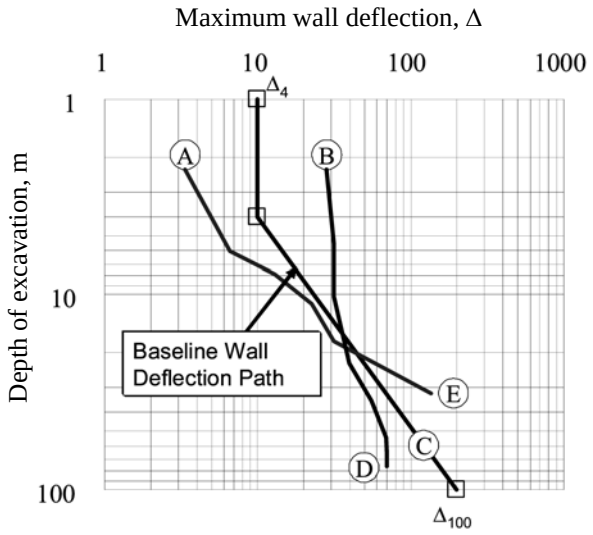

Fig. 2 Types of wall deflection paths

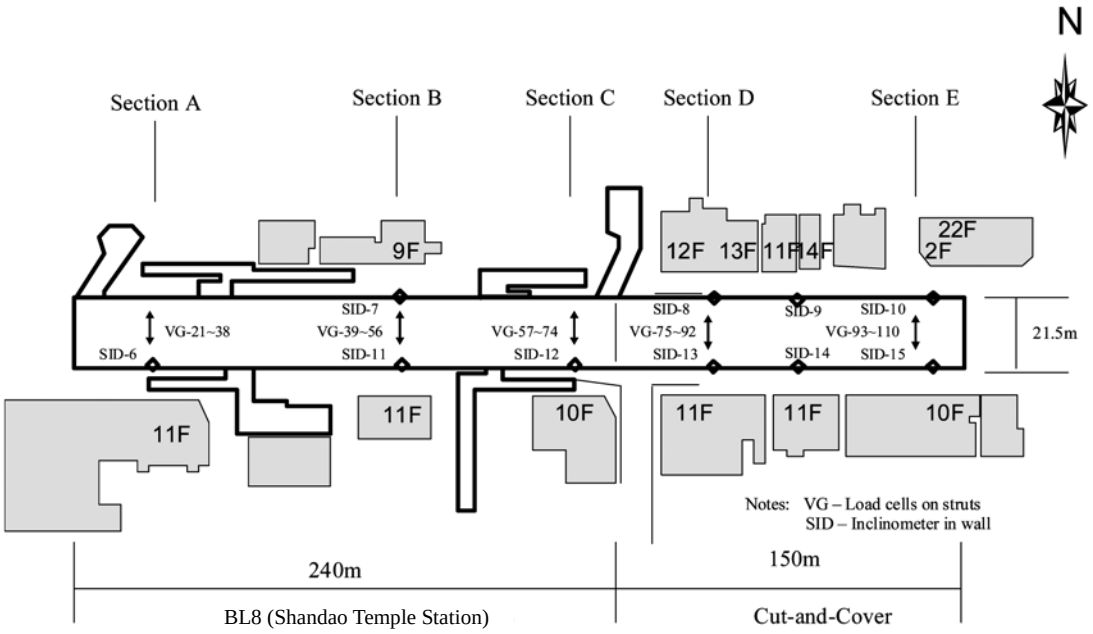

Fig. 3 Configuration of Shandao Temple Station (BL8 Station) and locations of instruments

Excavation was carried out to a maximum depth of 18.5 m in 7 stages as depicted in Fig. 4 and the pit was retained by diaphragm walls of 1m in thickness and propped by steel struts at 6 levels. There were 5 research sections, *i.e.*, Sections *A* through *E*, in which inclinometers were installed in the diaphragm walls for monitoring wall deflections and strain gages were mounted on all the struts for measuring strut loads so wall deflections can be correlated with changes in the lengths of struts. It has been reported that, because inclinometers were installed only to the bottom level of the wall, *i.e.*, depth of 30.5 m below ground surface, considerable movements occurred at the toes and readings obtained had to be corrected to account for these toe movements (Hwang *et al*. 2006; 2007b; Hsiung and Hwang 2009b).

The station is located near the center of the T2 Zone (Moh and Associates 1987; Lee 1996) and the ground conditions at this site are representative of the ground conditions in the T2 Zone. The 6 sublayers in the Sungshan Formation are clearly identifiable as depicted in Fig. 4. The Sungshan Formation is underlain by the Chingmei Formation at a depth of 50 m or so. The Chingmei Formation consists of gravels and coarse sand and is very permeable. It is a water-rich underground reservoir and was a major source of water supply for the city for years. As depicted in Fig. 5, the piezometric level in the Chingmei Formation was once lowered to EL.–40 m, or a depth of 44 m below ground

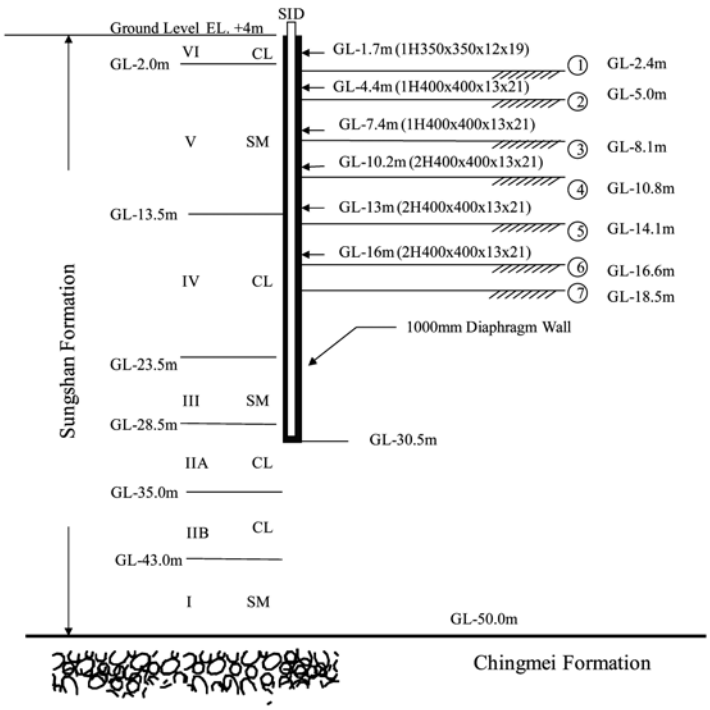

Fig. 4 Excavation scheme and ground conditions

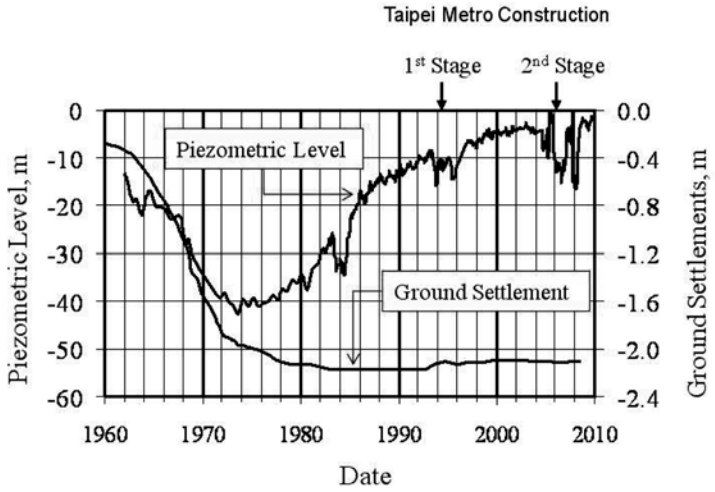

Fig. 5 Piezometric level in the Chingmei Formation and surface settlements in central city area of Taipei

surface, as a result of excessive pumping leading to a maximum ground settlement of 2.2 m due to consolidation in all the sublayers in the overlying Sungshan Formation. The piezometric level in the Chingmei Formation gradually recovered since mid-70's as pumping was banned. However, the recovery of piezometric level was interrupted by the underground construction of several major infrastructures, such as Taipei Metro, High-Speed Rail, and TRA (Taiwan Railways Administration) rails. At the time the excavation was carried out in the period of 1991 to 1994, the piezometric levels in the Chingmei Formation were, roughly, at a depth of 14 m below ground surface.

Back analyses were conducted to calibrate the soil parameters to be adopted in numerical analyses so wall deflections can be predicted in the future. This was achieved by comparing the results obtained in back analyses with the observed performance of walls. For the case of interest, analyses were performed by using the finite element program PLAXIS (PLAXIS BV, 2011) developed at Delft University and made available commercially by PLAXIS BV of the Netherlands. Figure 6 shows the finite element mesh adopted in the analyses. Since the Chingmei Formation is a competent stratum and ground movements therein are expected to be small, the base of the finite element mesh was assumed at the top of this formation. There were a total of 827 elements and 7,067 nodes in the mesh.

Soils were modeled by 15-node elements. The Mohr-Coulomb model was adopted for simulate the behavior of soils in all the subsoils. Clayey materials, *i.e.*, Type CL soils, were assumed to be undrained materials and sandy materials, *i.e.*, Type SM soils, were assumed to be drained materials. Effective stress analyses were performed for both types of soils. The Young's moduli of soils, *i.e.*, the so-called E values, were estimated as follows:

$$E' = 500\ S_u \tag{1}$$

$$E' = 2N\ (\text{MPa}) \tag{2}$$

in which S_u = undrained shearing strength and N = blow counts in standard penetration tests (SPT). Regarding the shearing strength of clayey materials, PLAXIS offers the option of adopting undrained shear strength, *i.e.*, $\Phi = \Phi_u = 0$ and $c = c_u$ (S_u is adopted herein) in effective stress analyses. The soil parameters adopted in the analyses are summarized in Table 1. The distribution of groundwater pressures acting on the outer face of the diaphragm wall is shown in Fig. 7. The water level inside the pit was assumed at a depth of 1m below the bottom in each stage of excavation.

The diaphragm walls were simulated by plate elements and an E value of 25,000 MPa was adopted for concrete with a f_c' value of 280 kgf. The EI (I = moment of inertia) and EA (A = sectional area) values of the diaphragm walls were reduced by 30%, giving a value of 1,464 MN × m for the former and 17,570 MN/m for the later, following the normal practice to account for the influence of tremieing and degradation of concrete during excavation. Struts were installed at a horizontal spacing of 4.5 m and all the struts were pre-loaded to 50% of their design loads. They were simulated by anchor-to-anchor rods and an E value of 210,000 MPa was adopted. Table 2 shows the stiffness of struts at various levels.

The deflections of the walls and the lateral movements of soils below the toe of the wall obtained from the analyses are shown in Fig. 8. The results have to be compared with observed wall deflections for confirming their validity. However, the final wall deflections interpreted from inclinometer readings, as depicted in Fig. 9, are drastically different. It is doubtless that different conclusions will be reached if different sets of readings are selected for comparison. Furthermore, as mentioned above, because buildings adjacent to the excavation were not included in the finite element model, it will be more meaningful to compare the wall deflection path obtained from the analyses with the baseline wall deflection path, rather than individual wall deflection profiles, provided that the baseline wall deflection path is available.

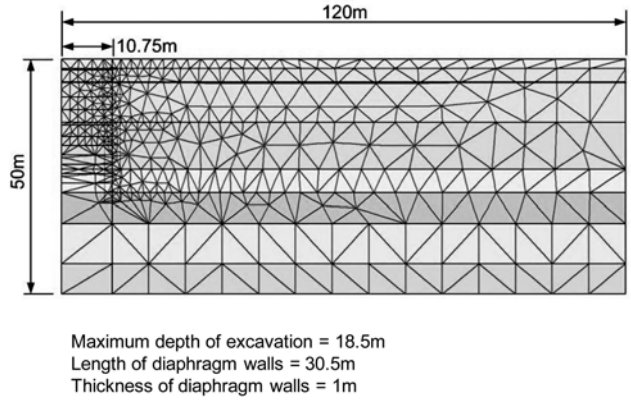

Fig. 6 Finite element model adopted in PLAXIS analyses

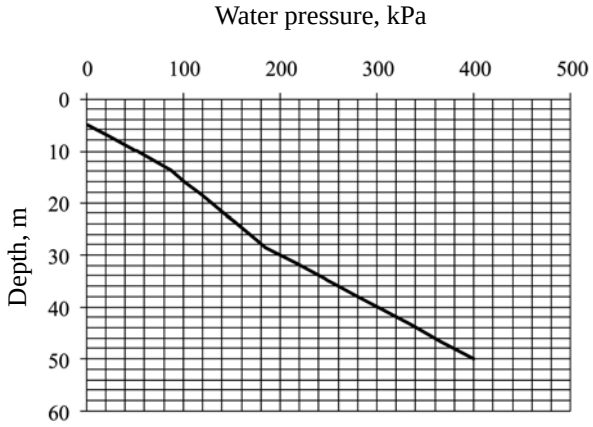

Fig. 7 Groundwater pressures on the outer face of diaphragm wall

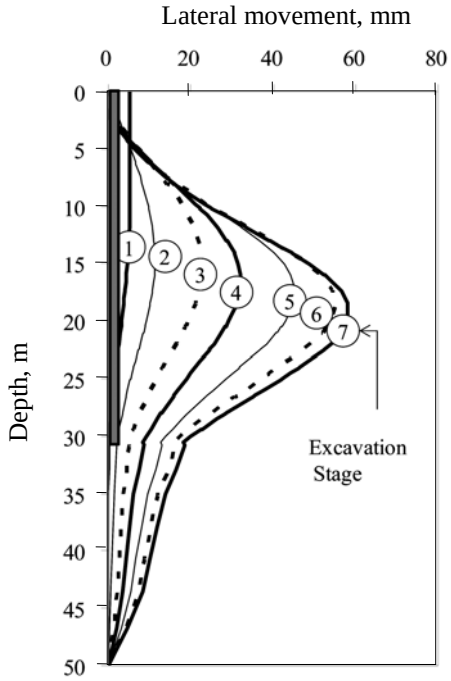

Fig. 8 Results of PLAXIS analyses

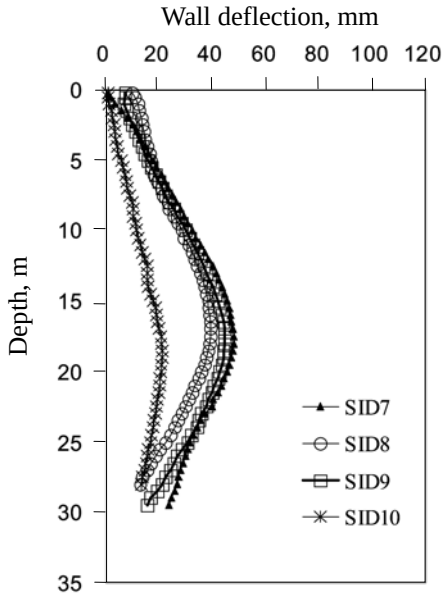

(a) Northern Wall

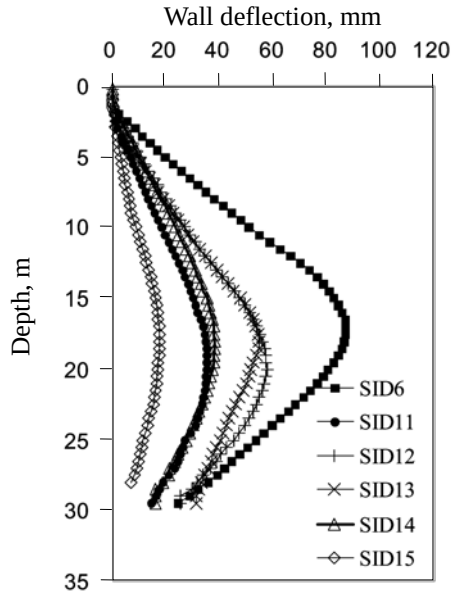

(b) Southern Wall

Fig. 9 Final inclinometer readings

Table 1 Soil properties and soil parameters adopted

Depth (m)	Soil Type	γ_t (kN/m^3)	N (blows)	S_u (kPa)	c' (kPa)	Φ' (deg)	E' (MN/m^2)	Poisson's Ratio, υ'
0 ~ 2	CL	18.6	3	20			10	0.35
2 ~ 13.5	SM	18.4	8	–	0	33	16	0.35
13.5 ~ 23.5	CL	18.8	6	40			20	0.35
23.5 ~ 28.5	SM	19.3	18	–	0	32	36	0.35
28.5 ~ 35	CL	19.4	17	150			75	0.35
35 ~ 43.5	CL	19.4		200			100	0.35
43.5 ~ 50	SM	21.6	30	–	0	35	60	0.30

Table 2 Stiffness of struts adopted in numerical analyses

Level	Members	Sectional Area (cm^2)	Stiffness (MN/m)
1	1H350 × 350 × 12 × 19	1 × 173.9 cm^2	77.3
2, 3	1H400 × 400 × 13 × 21	1 × 218.7 cm^2	97.2
4, 5, 6	2H400 × 400 × 13 × 21	2 × 218.7 cm^2	194.4

Figure 10 shows a comparison of the wall deflection paths interpreted from the inclinometer readings, with toe movements duly accounted for, with the reference envelope for walls of 1 m in thickness for excavations in the T2 Zone. Since the structures adjacent to the excavation and the annex attached to the station box, refer to Fig. 3, tend to reduce wall deflections, these wall deflection paths will mostly belong to Type A, refer to Fig. 2. In theory, the envelope of the wall deflection paths will approach the baseline wall deflection path as more and more cases are included. Therefore, as an alternative, the performance of the walls will better be studied by comparing the results obtained from analyses with the reference envelope before the baseline wall deflection is established.

Some of the wall deflection paths deviate from the reference envelope with good reasons and should be excluded from the comparison. For example, inclinometers SID10 and SID15 were very close to the end walls of the station and wall deflections observed were thus smaller because of the corner effects. Although inclinometer SID6 was also very close to the corner, jet grouting was carried out to stop the leakage on the wall in the 4th stage of excavation and caused excessive inward movements of the wall. Figure 11 shows the maximum wall deflections obtained from the PLAXIS analyses and, as can be noted, the relationship between the maximum wall deflection and depth of excavation does become more or less linear after excavation proceeds beyond a depth of 10 m as suggested in Moh and Hwang (2005). Such a relationship is shown as Type C deflection path in Fig. 2. The idealized wall deflection path, which was established by considering mainly the data points in the range of excavation depths of 10 m to 20 m, can be represented by Δ_4 = 10 mm and Δ_{100} = 500 mm. As can be noted from the figure, this idealized wall deflection path is sufficiently close to the reference envelope for 1 m walls in the T2 Zone previously established based on observations. In fact, it fits better the data points shown in Fig. 1. It is therefore suggested that this idealized wall deflection path be considered as the baseline wall deflection path for 1 m walls for excavations carried out by using the bottom-up method of construction in the T2 Zone.

As can be noted from Figs. 9 and 10, even with SID6, SID10 and SID15 excluded, the readings obtained by the rest of inclinometers are still very divertive. Amongst them, the readings from inclinometer SID12 were the largest and, presumably, were least affected by adjacent structures. Therefore, they were adopted for validating the results obtained by PLAXIS analyses. As shown in Fig. 12, the computed wall deflections in the last 2 stages of excavation are very close to what was recorded by inclinometer SID12. The computed wall deflections in earlier stages are larger than what was recorded for two possible reasons: Firstly, wall deflections were reduced by the presence of adjacent structures, particularly the entrance walls next to this inclinometer as shown in Fig. 3, and secondly, soil moduli could have been underestimated in the early stages of excavation because the Mohr-Coulomb Model was adopted in the PLAXIS analyses.

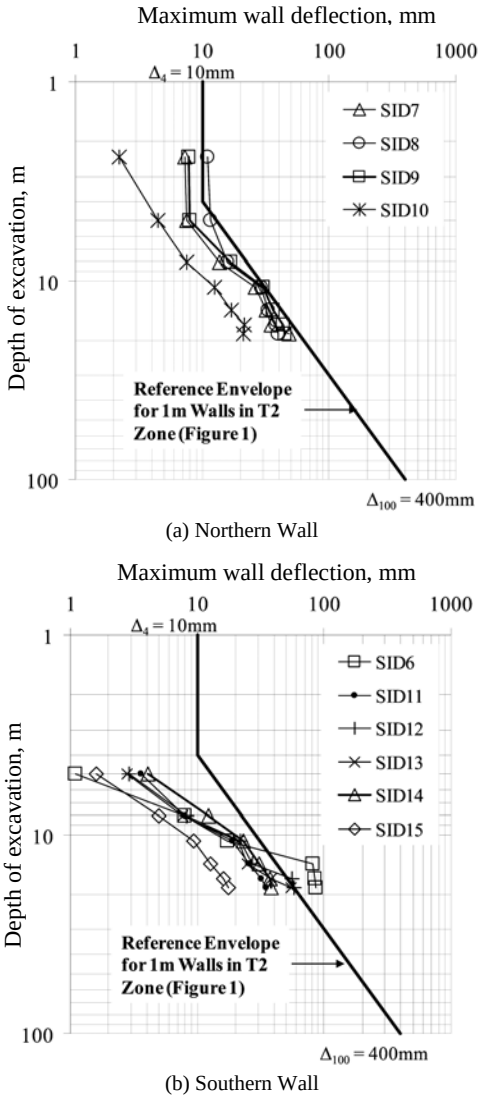

Fig. 10 Observed wall deflection paths as compared with the reference envelope

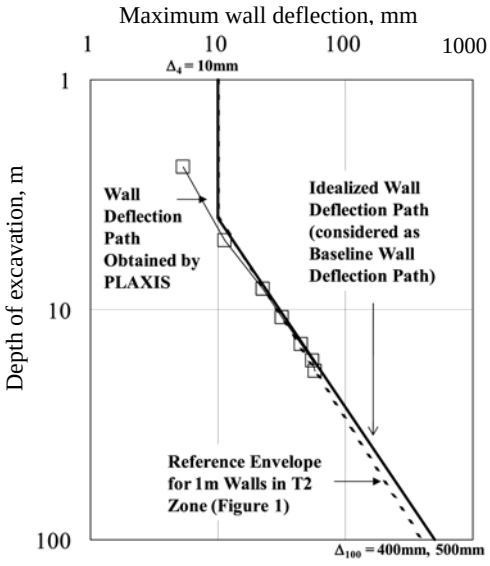

Fig. 11 Comparison of idealized wall deflection path with reference envelope in the T2 Zone

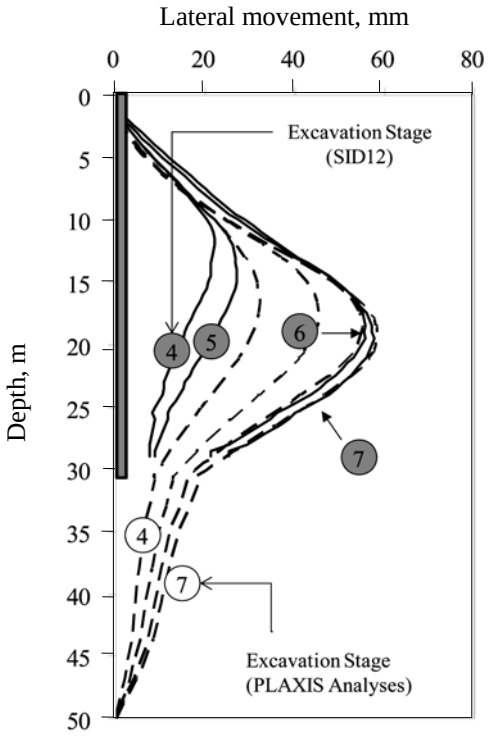

Fig. 12 Comparison of computed results with inclinometer readings

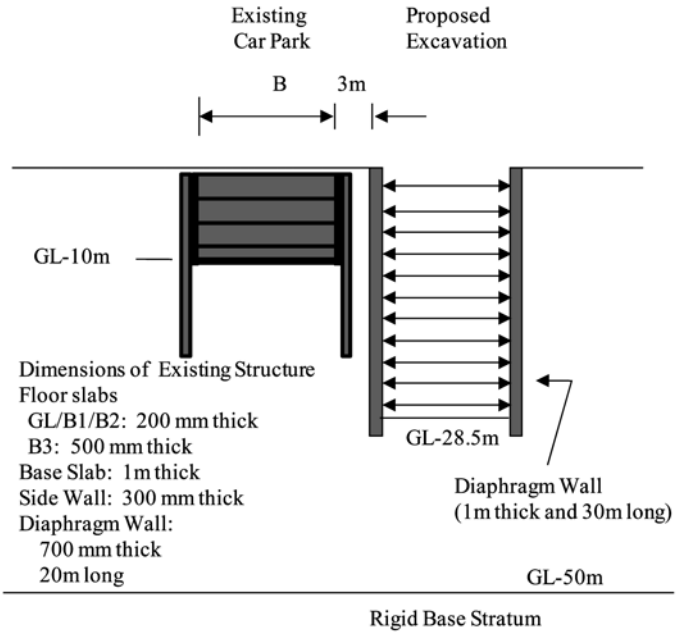

Fig. 13 Case 1 – Excavation next to an underground car park

4. TYPES OF WALL DEFLECTION PATHS

The excavation for Shandao Temple Station is used herein as an example to illustrate the applications of the concept of wall deflection path for evaluating the performance of walls. In all the cases discussed, the sequence of excavation and the structural elements are the same as discussed above. However, instead of stopping at a depth of 18.5 m, excavation was assumed to continue till a depth of 28.5 m with a 2 m increment in each stage subsequently in order to test the convergence of numerical process and the stability of the walls. The struts for these additional stages were of the same sizes as those for Levels 4, 5, and 6, refer to Table 2 for details.

Type C wall deflection path has already been demonstrated in Fig. 11. Four cases were analyzed with different scenarios to illustrate Types A and B deflection paths which indicate the influences of adjacent structures on wall deflections. Types D and E deflection paths indicate toe stabilities and are studied by varying the strength of soils in Sublayer II.

4.1 Excavations next to Underground Structures – Type A Wall Deflection Paths

Figure 13 shows the configuration of Case 1 in which the excavation is to be carried out next to an underground structure, for example, a 3-level car park. The diaphragm walls left in place after the completion of the car park are 700 mm in thickness and 20 m in length. For simplicity, the car park was assumed to have existed for a sufficiently long period for the ground to stabilize and the construction process of the car park was thus not simulated in the analyses. The structural members of car park together with the associated diaphragm walls were put into the ground at the same time after the geo-stresses were initialized.

As can be noted from Fig. 14(a), the maximum wall deflections obtained from the PLAXIS analyses for early stages of excavation for the wall immediately next to the car park are smaller than those shown by the baseline deflection path and the differences between the two diminish as the depth of excavation increases. The wall deflection path for this wall is a typical Type A deflection path. Wall deflections increase at reducing rates, in the log-log plot, after the depth of excavation of 18.5 m because of the constraint of the rigid base and the deflection path resembles Type D path which will be discussed in detail in Section 4.4. The deflections for the wall on the opposite side of the excavation, however, appear to be unaffected and the deflection path is very close to the baseline wall deflection path for depths of excavation varying from 10 m to 18.5 m.

The influence of the car park on wall deflections is not as pronounced as one would expected based on observation, refer to Fig. 10. An on-going study has shown that the results of analyses are insensitive to the rigidity of the structure of the car park. Therefore, the reduction in wall deflection is presumably due to the reduction of soil mass.

To investigate the effects of the sizes of adjacent underground spaces on wall deflection paths, analyses were performed for the case in which the width of the car park was increased from 20 m to 40 m and the results obtained are given in Fig. 14(b). The influence of the car park has somewhat increased and the wall deflection path does become flatter, but still not to the extent observed in Fig. 10. The large differences between the observed deflection paths and the reference envelope shown in Fig. 10 is presumed to be caused by other factors, in addition to the use of Mohr-Coulomb model, such as corner effects and the increase in wall stiffness due to annexed structures.

To further investigate the effects of the sizes of adjacent underground spaces on wall deflection paths, analyses were performed for Case 2, as shown in Fig. 15, in which the excavation is to be carried out next to a much larger underground structure, for example a 3-level metro station. Except for the geometry, the

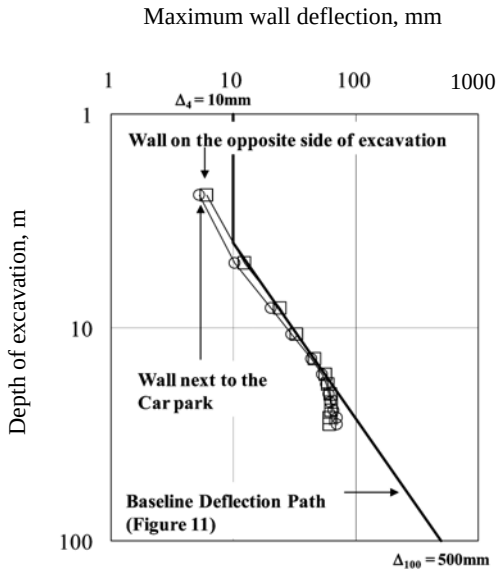

(a) B = 20 m

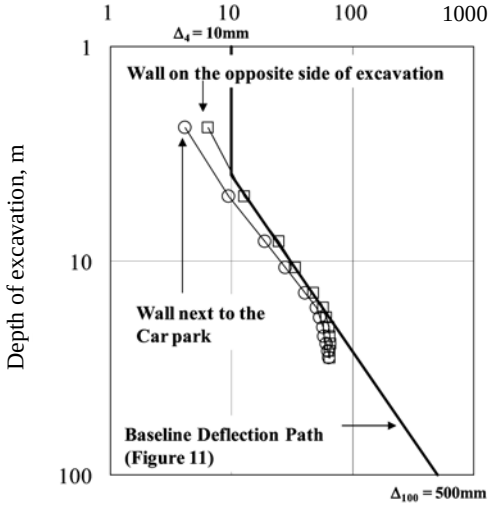

(b) B = 40 m

Fig. 14 Case 1 – Results of PLAXIS analyses

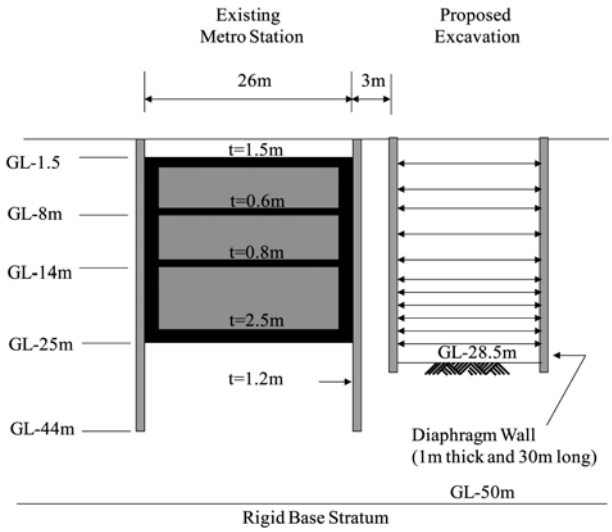

Fig. 15 Case 2 – Excavation next to an underground metro station

way the analyses were performed is the same as that for the car park. The results obtained are given in Fig. 16. The influence becomes much larger as can be noted by comparing Fig. 16, with Fig. 14. In the range of depth of excavation of 10 m to 20 m, the deflections for the wall immediately next to the station are now only about a half of what can be read from the baseline wall deflection path. The deflection path, for the wall on the opposite side of the excavation, however, is only slightly above the baseline wall deflection path.

What is of great interest is the fact that deflections for the wall next to the station not only reduce in rate of increase, but actually reduce in magnitude as excavation proceeds below a depth of 22.5 m, *i.e.*, in the last 3 stages of excavation. This is presumably due to the imbalance of earthpressure on the two sides of the excavation. A similar trend, but less pronounced, can also be observed in Fig. 14(a).

4.2 Excavation next to Surcharge Loads – Type B Wall Deflection Paths

Figure 17 shows the configuration of Case 3 in which the excavation is to be carried out next to surcharge loads, for example, an embankment. Distributed loads, q = 25, 50, 100 and 150 kPa, were added after geo-stresses were initialized, followed by the staged excavation in the same manner as described above. As shown in Fig. 18, the deflections of the wall next to the embankment increase as the distributed load from the embankment increases and the wall deflection paths resemble Type B paths. For depths of excavation greater than 10 m, wall deflections for a surcharge load of 150 kPa are about 3 times as much in comparison with what can be interpreted from the baseline wall deflection path. The imbalance of the loading on the two sides, however, reduces the wall deflections on the opposite side of the excavation and the wall deflection paths resemble Type A paths for shallow depths. For great depths of excavation, the wall deflection paths resemble Type D paths and wall deflections not only reduce in rates but also drastically reduce in magnitudes.

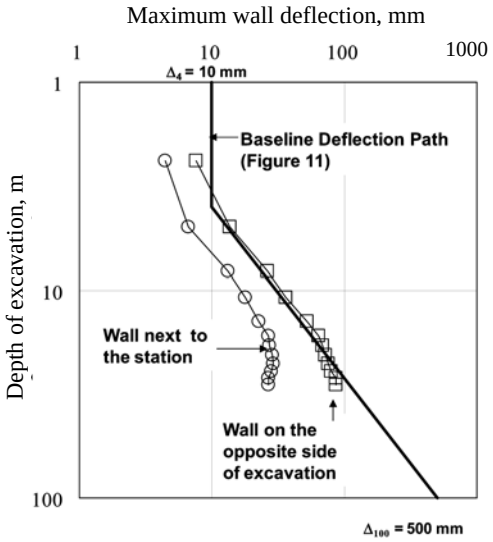

Fig. 16 Case 2 – Results of PLAXIS analyses

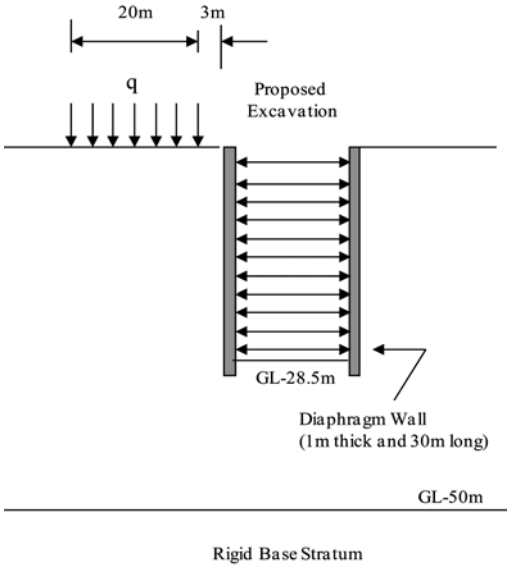

Fig. 17 Case 3 – Excavation next to an embankment

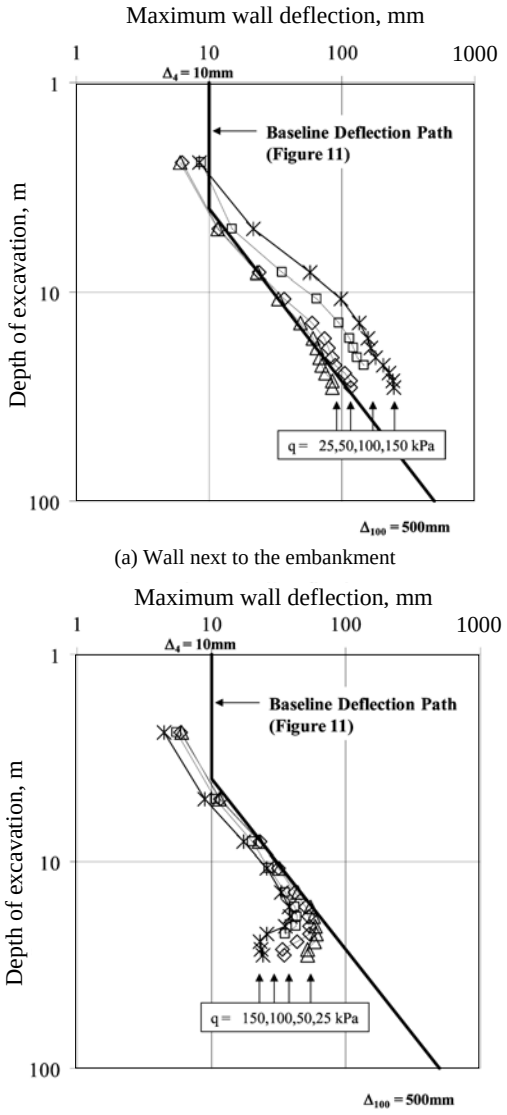

Fig. 18 Case 3 – Results of PLAXIS analyses

4.3 Excavations next to Highrise Buildings – Type A or B Wall Deflection Paths

Figure 19 shows the configuration of Case 4 in which the excavation is to be carried out next to a highrise building with a 3-level basement founded at a depth of 10 m below surface. It is evident that the influence of the building on wall deflections is a combination of the influence of two mutually compensating factors, *i.e.*, the basement and the super structure, and is, therefore, the net of the results of the two mechanisms illustrated in Case 1 and Case 3.

To be able to compare the results obtained with those obtained for Cases 1 and 3, the basement is assumed to have the same configuration as the car park studied in Case 1 and the superstructure is assumed to have the same width and the same loading as the embankment studied in Case 3. The basement and the superstructure were added to the finite element mesh after geo-stresses were initialized. The excavation scheme was the same as that adopted in Cases 1, 2 and 3. The weight of soil mass replaced by the basement is equivalent to a distributed load of about 184 kPa and the weight of the basement structure, including the weight of diaphragm wall, is equivalent to a distributed load of about 132 kPa, giving a net reduction of 52 kPa which is compensated by the load from the superstructure of the building varying from 50 kPa to 150 kPa.

As can be noted from Fig. 20(a), for the wall immediately next to the building, deflections increase as the load from the superstructure increases and the data points match the baseline deflection path for a distributed load of 50 kPa which well agrees with the deficit in soil weight. It is thus concluded that that wall deflection paths will belong to Type A if the weight of the building (including superstructure and substructure) is less than the weight of soil mass replaced, and Type B otherwise. The wall deflections for the wall on the opposite side of the excavation, however, were only slightly affected as depicted in Fig. 20(b).

4.4 Toe Stability – Type D or E Wall Deflection Paths

The key to the toe stability of the wall is the strength of Sublayer II, refer to Fig. 4, in the Sungshan Formation. In contrast to the clays in the K1 Zone, the strengths of the clays in the

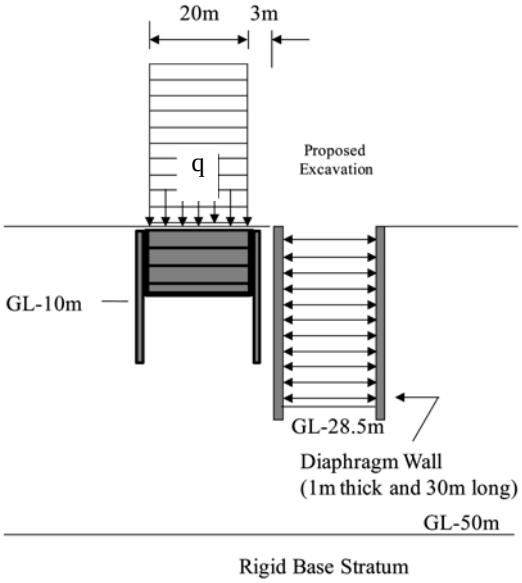

Fig. 19 Case 4 – Excavation next to highrise buildings

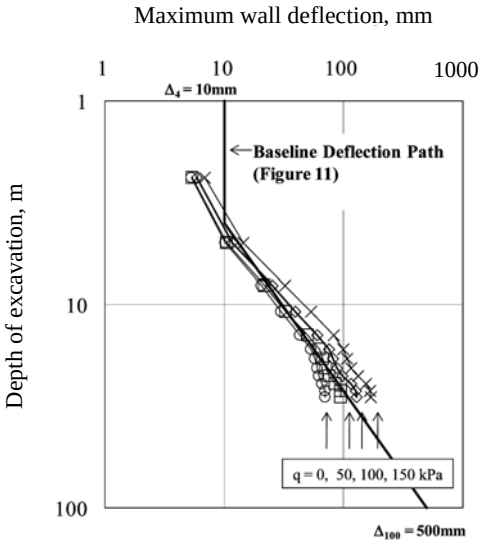

(a) Wall next to the building

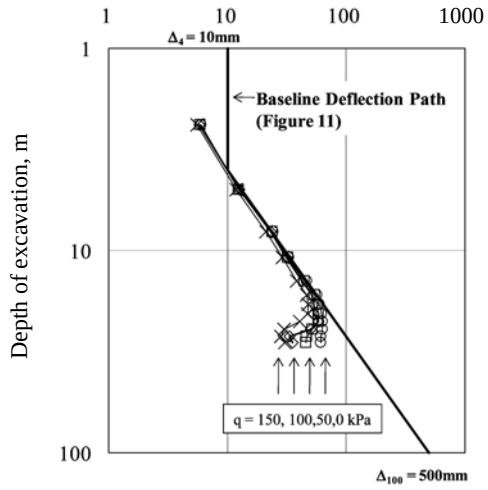

(b) Wall on the opposite side of excavation

Fig. 20 Case 4 – Results of PLAXIS analyses

T2 Zone received much less attention in the past. The shearing strength of Taipei clay obtained in CKoUC tests (K_o-consolidated undrained triaxial compression tests) can be estimated by using the so-called SHANSEP equation (Ladd and Foote 1974; Ladd and deGroot 2003) as follows (Chin *et al.* 1994; 2006):

$$S_u / \sigma_{vc}' = 0.32\ (OCR)^{0.82} \tag{3}$$

in which σ_{vc}' = effective overburden pressure, OCR = over-consolidation ratio. The piezometric level of groundwater in the Chingmei formation was a few meters above the ground level in the first half of the 20th century (Wu 1968). For practical purposes, it can be assumed at the ground level as the initial condition. It dropped to a depth, as much as, 44 m below ground surface in the 70's and remained at this depth for years as indicated in Fig. 5. As a result, all the subsoils in the Sungshan Formation in the T2 Zone were substantially consolidated. This is particularly true for Sublayer II because the underlying Sublayer I is very permeable and the piezometric level in Sublayer I was practically the same as the piezometric level in the Chingmei Formation. The shearing strength, S_u, of Sublayer II at a depth of 40 m, for example, increased from the initial value of 108 kPa to 236 kPa as depicted in Table 3. Although it was somewhat reduced as the piezometric level rose in the 90's when the excavation for Shandao Temple Station was carried out, with a value of 218 kPa, it was still twice the initial value. Therefore the soil below the bottom of excavation was very stable and provided sufficient resistance to toe movements for the case of interest and, as can be noted from Fig. 21, the wall deflections would increase at a reducing rate in the log-log plot subsequently, giving a Type D deflection path if excavation continues below the depth of 18.5 m.

Suppose the piezometric level of groundwater in the Chingmei Formation had never dropped, the shearing strength of Sublayer II would have only been, roughly, a half of what it was in the 90's. To see whether the diaphragm wall would still be stable in such a case, analyses were carried out by reducing the strength of Sublayer II shown in Table 1 by a half. The toe movements of the diaphragm wall would increase rather rapidly subsequent to the 8th stage of excavation, with a depth of excavation of 20.5 m, as shown in Fig. 22 and the wall deflection path would become Type E as shown in Fig. 21.

It should be pointed out, however, the case analyzed is hypothetic and there is no precedence for excavations to exceed a depth of 18.5 m with walls of only 30.5 m in length. Seepage was not considered in the analyses presented herein and blow-in and piping may become governing, particularly as the piezometric level in the Chingmei Formation has considerably risen in recent years. Secondly, Sublayer II was assumed to be an undrained material with its strength unchanged but, in reality, may lose its strength during excavation due to relaxation of geo-stress and seepage.

5. PARAMETRIC STUDY

The factors affecting the performance of diaphragm walls are numerous and it is certainly not possible to include all of them in this study. Among them, soil moduli, stiffness of wall, and width of excavation are the major ones with dominating influences and their influences on wall deflections are studied herein by using the concept of wall deflection path.

5.1 Sensitivity of Soil Moduli on Wall Deflection Paths

Figure 23 shows the results of PLAXIS analyses for 3 sets of soil moduli as follows:

Set A: Soil moduli were obtained by using Eqs. 1 and 2 and the values are given in Table 1. The idealized wall deflection path obtained from the analyses is presumed to be the baseline wall deflection path.

Set B: The soil moduli are a half of those in Set A

Set C: Soil moduli are twice those in Set A.

As can be noted, the Δ_4 values for the idealized deflection paths are, roughly, inversely proportional to soil moduli while the Δ_{100} values are the same for all the 3 sets. This finding is consistent with what was reported in Hsiung and Hwang (2009c). It makes adjustment of Δ_4 values much easier, if necessary. In this regard, it should be emphasized again that idealized wall deflection paths are established mainly based on the data for depths of excavation in the range of 10 m to 20 m.

Table 3 Undrained shearing strength of Sublayer II

Period	Overburden Pressure (kPa)	Piezometric Level	Porewater Pressure (kPa)	Effective Overburden Pressure (kPa)	OCR	Undrained Shear Strength (kPa)
Initial	756	GL +0 m	400	356	1	114
70's	756	GL-40 m	0	756	1	242
90's	756	GL-14 m	260	496	1.52	224

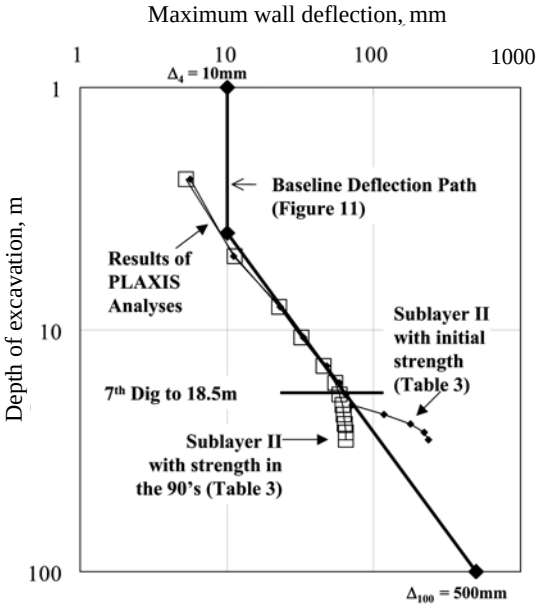

Fig. 21 Influence of consolidation of Sublayer II on wall deflection path

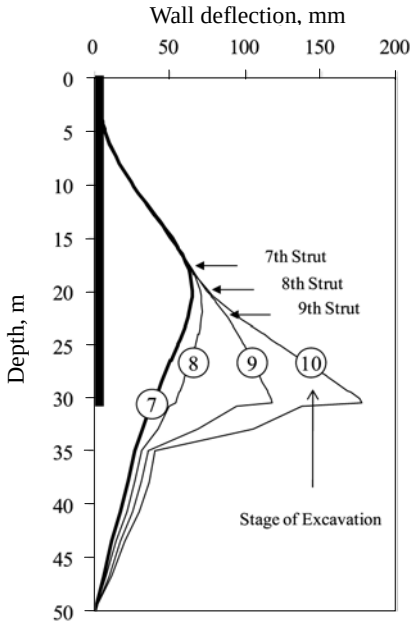

Fig. 22 Wall deflections if groundwater had not been lowered

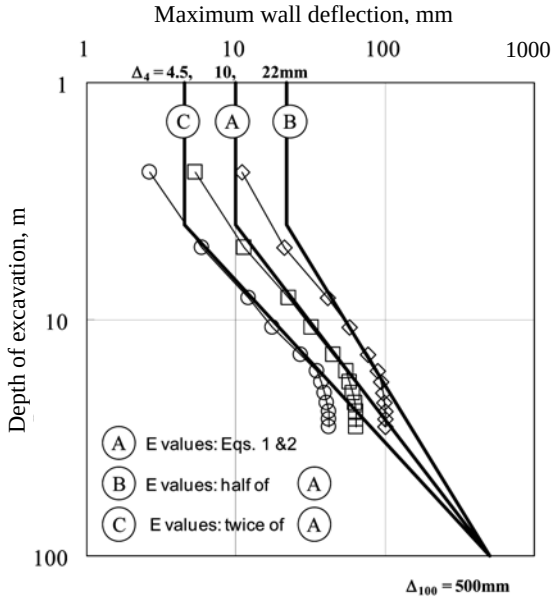

Fig. 23 Influence of soil moduli on wall deflections

5.2 Sensitivity of Wall Stiffness on Wall Deflection Paths

Analyses were performed for walls with thicknesses of 0.6 m, 1 m and 1.5 m, of which the, *EI* and *EA* values are given in Table 4. As can be noted from Fig. 24, the Δ_{100} values for the idealized deflection paths are 300 mm, 500 mm and 1000 mm, respectively while the Δ_4 values are the same for all these walls. Figure 25 shows the relationship between the Δ_{100} and the *EI* (*E* = Young's modulus and *I* = moment of inertia) values of walls. The Δ_{100} values for walls with various thicknesses can be obtained directly from the figure. It however should be noted that an *E* value of 25,000 MPa was adopted for these walls in the PLAXIS analyses together with a reduction factor of 0.7 on the *EI* values.

5.3 Sensitivity of Width of Excavation on Wall Deflection Paths

Analyses were performed for various widths of excavation and, as shown in Fig. 26 and Table 5, the influence the width of excavation on wall deflections is quite significant and should not be overlooked. The Δ_4 values for the idealized deflection paths vary from 4 mm for excavations of 10 m in width to 24 mm for excavations of 80 m in width. Fortunately, the Δ_{100} values are more or less unaffected.

6. BASELINE WALL DEFLECTION PATH

Based on the foregoing discussions, it is clear that wall deflections are affected by too many factors and it is essential to establish baseline wall deflection paths for various ground conditions so the influences of various factors can be quantified. Baseline wall deflection paths have been grossly defined as the wall deflection paths for excavations carried out by using the bottom-up method of construction in green field without being influenced by adjacent structures. Such a definition is certainly not sufficiently precise for the purpose and has to be refined, as follows, to avoid confusions:

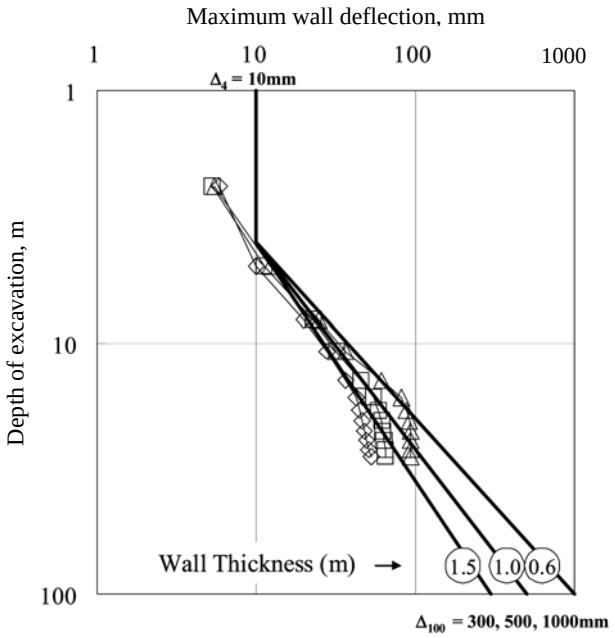

Fig. 24 Influence of wall stiffness on wall deflections

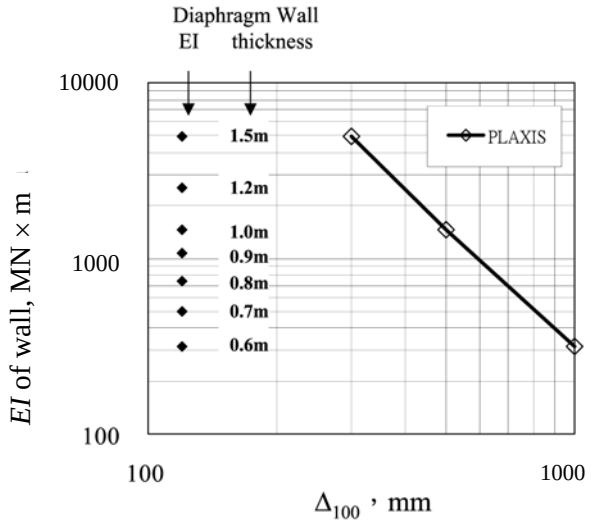

Remarks: **(1) E = 25,000 MPa**
(2) Reduction factor for EI = 0.7

Fig. 25 Influence of wall stiffness on Δ_{100} values

Table 4 Stiffness of walls with different thicknesses

Thickness (m)	EI (MN × m)	EA (MN/m)
0.6 m	316	10,542
1.0 m	1,464	17,570
1.5 m	4,941	26,355

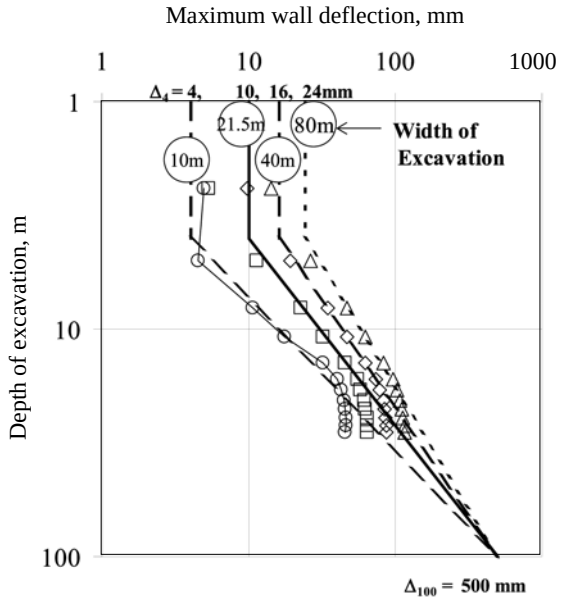

Fig. 26 Influence of width of excavation on wall deflections

Table 5 Maximum wall deflections for various widths of excavations

Depth of Excavation	Width of Excavation			
	10 m	20 m	40 m	80 m
10 m	16 mm	30 mm	43 mm	57 mm
20 m	45 mm	71 mm	89 mm	110 mm

a. Since walls of 1m in thickness are most common, it is suggested that baseline wall deflection paths refer to the idealized deflection paths for 1 m walls.

b. Since most excavations for metro stations and cut-and-cover tunnels vary from 15 m to 25 m in width, it is suggested baseline wall deflection paths refer to the idealized deflection paths for excavations of 20 m in width.

Wall deflection paths for walls of various thicknesses and excavations for various widths can be deduced from the baseline wall deflection paths, following the rationales given above, once they become available.

It should be pointed out that the analyses presented herein were performed by adopting the Mohr-Coulomb model to simulate the nonlinear behavior of soils. The wall deflection paths obtained will be somewhat different if different material models are adopted. However, since the results of analyses have been verified with the observation, the baseline deflection path established is believed to be valid for practical purposes.

7. CONCLUDING REMARKS

The foregoing discussions lead to the following conclusions:

1. Wall deflections are affected by many factors and it is important to establish baseline wall deflection paths so the influence of various factors can be quantified.

2. Baseline wall deflection paths are defined as the idealized wall deflection paths for excavations of 20 m in width with diaphragm walls of 1 m in thickness carried out in green field by using the bottom-up method of construction.
3. For the T2 Zone in the Taipei Basin, the baseline wall deflection path obtained by adopting the Mohr-Coulomb model for soils can be represented by $\Delta_4 = 10$ mm and $\Delta_{100} = 500$ mm.
4. The adoption of the Mohr-Coulomb model, together with the use of $E' = 500\ S_u$ for clays and $E' = 2N$ (in MPa) for sands, appears to lead to reasonable results as far as wall deflections are of concern.

It should be noted, however, there are numerous factors affecting the performance of diaphragm walls and, therefore, the results presented herein are subjected to the limitation that excavations are carried out to the normal practice and normal workmanship on Taiwan, particularly, in the Taipei Basin.

REFERENCES

Chao, H. C, Chang, J. F., and Hwang, R. N. (2010). "Evaluation of performance of diaphragm walls in deep excavations by using deflection path method." *17th Southeast Asian Geotechnical Conference*, Taipei, Taiwan, **1**, 390–393.

Chin, C. T., Crooks, A. J. H., and Moh, Z. C. (1994). "Geotechnical properties of the cohesive Sungshan deposits, Taipei" *Geotechnical Engineering Journal*, Southeast Asian Geotechnical Society, 77–103.

Chin, C. T., Chen, J. R., Hu, I. C., Yao, T. C., and Chao, H. C. (2006). "Engineering characteristics of Taipei clay." *Proc., 2nd International Workshop on Characterization and Engineering Properties of Natural Soils*, Singapore.

Hsiung, B. B. C. and Hwang, R. N. (2009a). "Influence of ground improvement on deflection of diaphragm walls in deep excavations." *Int. Sym. on Ground Improvement Technologies and Case Histories*, Singapore, 305–310.

Hsiung, B. B. C. and Hwang, R. N. (2009b). "Correction of inclinometer readings for toe movements." *Special Issue on Excavation and Tunneling in Geotechnical Engineering*, SEAGS, 39–48.

Hsiung, B. B. C. and Hwang, R. N. (2009c). "Evaluating performance of diaphragm walls by wall deflection path." *Special Issue on Excavation and Tunneling in Geotechnical Engineering*, SEAGS, 81–90.

Hwang, R. N. and Moh, Z. C. (2007a). "Performance of floor slabs in excavations using top-down method of construction and correction of inclinometer readings." *Journal of GeoEngineering*, TGS, **2**(3), 111–122.

Hwang, R. N. and Moh, Z. C. (2007b). "Deflection paths and reference envelopes for diaphragm walls in the Taipei Basin." *Journal of GeoEngineering*, TGS, **2**(1), 1–12.

Hwang, R. N. and Moh, Z. C. (2008). "Evaluating effectiveness of buttresses and cross walls by reference envelopes." *Journal of GeoEngineering*, TGS, **3**(1), 1–11.

Hwang, R. N., Moh, Z. C., and Kao, C. C. (2006). "Design and construction of deep excavations in Taiwan." Seminar on The State-of-the-Practice of Geotechnical Engineering in Taiwan and Hong Kong, Hong Kong.

Hwang, R. N., Moh, Z. C., and Kao, C. C. (2007a). "Reference envelopes for evaluating performance of diaphragm walls." *13th Asian Regional Conference*, Kolkatta, India, 505–508.

Hwang, R. N., Moh, Z. C., and Wang, C. H. (2007b). "Toe movements of diaphragm walls and correction of inclinometer readings." *Journal of GeoEngineering*, TGS, **2**(2), 61–72.

Hwang, R. N., Moh, Z. C., and Wang, C. H. (2007c). "Performance of retaining system in excavation for Core Pacific City." *Journal of GeoEngineering*, TGS, **2**(2), 53–60.

Ladd, C. and DeGroot, D. (2003). "Recommended practice for soft ground site characterization." Arthur Casagrande Lecture, *12th Panamerican Conference on Soil Mechanics and Geotechnical Engineering*, Massachusetts Institute of Technology, Cambridge, MA, U.S.A., 22–25.

Ladd, C. C. and Foote, R. (1974). "A new design procedure for stability of soft clays." *Journal of the Geotechnical Engineering Division. ASCE*, **100**(GT7), 763–786.

Lee, S. H. (1996). "Engineering Geological Zonation for the Taipei City." *Sino-Geotechnics*, **54** (in Chinese).

Moh, Z. C. and Hwang, R. N. (2005). "Geotechnical considerations in the design and construction of subways in urban areas." *Seminar on Recent Developments on Mitigation of Natural Disasters*, Urban Transportation and Construction Industry, Jakarta, Indonesia.

Moh and Associates (1987). "Engineering soil properties of the Taipei Basin." Project Report, 85043, Ret-Ser Engineering Agency and Taipei Public Works Department, Taipei, Taiwan (in Chinese).

PLAXIS BV (2011). *Reference Manual PLAXIS BV*: Amsterdam, the Netherlands.

Wu, C. M. (1968). "Subsidence in Taipei Basin, Part II." *Journal of the Chinese Institute of Civil and Hydraulic Engineering*, Taipei, Taiwan, **4**, 53–81.